



Article

Non-Linear Response of PM_{2.5} Pollution to Land Use Change in China

Debin Lu ¹ , Wanliu Mao ^{1,2,*}, Wu Xiao ¹ and Liang Zhang ³

¹ Department of Land Management, Zhejiang University, Hangzhou 310058, China; ludebin@zju.edu.cn (D.L.); xiaowu@zju.edu.cn (W.X.)

² Zhejiang Academy of Surveying and Mapping, Hangzhou 311100, China

³ School of Urban Construction, Zhejiang Shuren University, Hangzhou 310015, China; zhangliang0930@zju.edu.cn

* Correspondence: 11922077@zju.edu.cn

Abstract: Land use change has an important influence on the spatial and temporal distribution of PM_{2.5} concentration. Therefore, based on the particulate matter (PM_{2.5}) data from remote sensing instruments and land use change data in long time series, the Getis-Ord Gi* statistic and SP-SDM are employed to analyze the spatial distribution pattern of PM_{2.5} and its response to land use change in China. It is found that the average PM_{2.5} increased from 25.49 µg/m³ to 31.23 µg/m³ during 2000-2016, showing an annual average growth rate of 0.97%. It is still greater than 35 µg/m³ in nearly half of all cities. The spatial distribution pattern of PM_{2.5} presents the characteristics of concentrated regional convergence. PM_{2.5} is positively correlated with urban land and farmland, negatively correlated with forest land, grassland, and unused land. Furthermore, the average PM_{2.5} concentrations show the highest values for urban land and decrease in the order of farmland > unused land > water body > forest > grassland. The impact of land use change on PM_{2.5} is a non-linear process, and there are obvious differences and spillover effects for different land types. Thus, reasonably controlling the scale of urban land and farmland, optimizing the spatial distribution pattern and development intensity, and expanding forest land and grassland are conducive to curbing PM_{2.5} pollution. The research conclusions provide a theoretical basis for the management of PM_{2.5} pollution from the perspective of optimizing land use.

Keywords: particulate matter (PM_{2.5}); land use change; non-linear; spatial regression model



Citation: Lu, D.; Mao, W.; Xiao, W.; Zhang, L. Non-Linear Response of PM_{2.5} Pollution to Land Use Change in China. *Remote Sens.* **2021**, *13*, 1612. <https://doi.org/10.3390/rs13091612>

Academic Editor: Luke Knibbs

Received: 11 March 2021

Accepted: 19 April 2021

Published: 21 April 2021

Publisher's Note: MDPI stays neutral with regard to jurisdictional claims in published maps and institutional affiliations.



Copyright: © 2021 by the authors. Licensee MDPI, Basel, Switzerland. This article is an open access article distributed under the terms and conditions of the Creative Commons Attribution (CC BY) license (<https://creativecommons.org/licenses/by/4.0/>).

1. Introduction

The city is the densest place for human activities and is the space where air pollutants are most likely to accumulate [1,2]. Since the 1980s, with the rapid urbanization process and social and economic development, peoples' material wealth and living standards have been improved in China, but this has also brought a series of environmental problems [3,4]. Moreover, it highlights the serious contradiction between accelerating the urbanization process and abiding by ecological and environmental protection. Developed countries such as Europe and the United States have experienced air pollution problems for more than 100 years. Pollution increased intensively in China's economically developed regions in the past 20–30 years [5–8], especially PM_{2.5} (Particulate matter with aerodynamic diameter ± 2.5 µm) pollution [9–12]. At present, China has become one of the most polluted areas in the world in regards to PM_{2.5} pollution [1,11]. It is particularly prominent in the Beijing-Tianjin-Hebei region to the east of Hu Line, Yangtze River Delta, Chengdu-Chongqing Economic Zone, Guanzhong Economic Zone, Central Plains, and Harbin-Changchun urban agglomeration. They have become the worst-hit areas [1,9]. Furthermore, because PM_{2.5} can remain in the atmosphere for a longer time than PM₁₀ and total suspended particulate matter (TSP), and contains sulfates, nitrates, dust, polycyclic aromatic hydrocarbons, and heavy metals that are toxic to the human body [13], it significantly affects human

health [14,15], atmospheric visibility [16], climate change [17], and social and economic development [18]. Therefore, it has become an important environmental issue that prevents China from achieving urban Sustainable Development Goals (SDGs) by 2035.

The source analysis of PM_{2.5} pollution was emphasized in previous studies [19–23], and it was found that urban PM_{2.5} mainly came from domestic and industrial fire coal and automobile exhaust emissions [24–27]. However, rapid urbanization has led to changes in land use patterns and functions. Particularly, a large number of natural surfaces have been converted into artificial surfaces, lots of farmland and forest land are exploited, and land use types and patterns have undergone tremendous changes in several major urban agglomerations [28], such as the Beijing-Tianjin-Hebei region, Yangtze River Delta, Pearl River Delta, and Chengdu-Chongqing Economic Zone. Consequently, sources of atmospheric pollutants increased [29–32]. Meanwhile, changes in hydrothermal conditions can significantly affect the spatial and temporal distribution pattern of PM_{2.5} [33,34]. On the one hand, the land is the underlying surface of the atmosphere. The composition and pattern of land use types can directly affect PM_{2.5} [35,36] because different land use types carry different intensities of human activities, which also means different pollution emissions. Further, changes in the landscape structure can cause changes in the local climate [37], thereby affecting the migration and conversion of PM_{2.5}. Significantly, land use changes at the regional or macro scale can affect climate conditions. Therefore, the land is the foundation for carrying everything, and land use change has a significant impact on regional energy flow, substance circulation, and biological processes. This is an important reason for a series of urban environmental problems [38,39].

At present, the studies on the relationship between PM_{2.5} and land use change mostly focus on large developed cities or a more microscopic scale [40,41]. Due to the atmospheric transport of atmospheric pollution, urban PM_{2.5} pollution is not only related to local emissions, but also to regional and long-range transport, which has a certain contribution [31,35,42,43]. Local and regional land use changes will directly or indirectly affect the local PM_{2.5}. In addition, PM_{2.5} and influencing factors constitute a complex non-linear dynamic system. There are multi-level scale structures and local changes in the time domain [44,45]. The complex process of non-linear interaction and response cannot be revealed in traditional linear analysis methods. However, non-linear numerical modeling methods are used in other studies to study air pollution diffusion and distribution patterns [46–48]. Land use is utilized as a predictive factor, and the response of PM_{2.5} to land use changes is not the focus of their research. Therefore, it is necessary to develop a non-linear model to study the response mechanism of PM_{2.5} to land use changes in a large area.

Thus, based on the PM_{2.5} dataset (from remote sensing instruments and not from ground-based measurement networks) and land use change data in long time series, the Getis-Ord G_i^* statistic (Pronounced G-i-star) and the semi-parametric spatial Durbin model (SP-SDM) are employed to analyze the spatial distribution pattern of PM_{2.5} and its response to land use change. The resultant z -scores and p -values of the Getis-Ord G_i^* statistic can reveal spatial clusters of PM_{2.5} with either high or low values, and the SP-SDM model shows the non-linear characteristics of PM_{2.5} response to land use change. It provides a theoretical reference to improve urban air quality by optimizing land use methods to promote the realization of Chinese cities' SDGs by 2035.

2. Materials and Methods

2.1. Data

2.1.1. PM_{2.5} Dataset

China Regional Estimates (V4.CH.03) PM_{2.5} dataset was downloaded from (http://fizz.phys.dal.ca/~atmos/martin/?page_id=140 accessed on 1 March 2020). This dataset was produced by the Atmospheric Environmental Analysis Group of Dalhousie University. The spatial resolution is $0.01^\circ \times 0.01^\circ$ (where the 0.01 arc division is about 1 km measured at the equator), and the time span is from 2000 to 2016. It has good data quality and can verify

that R^2 is 0.81 [9]. Van Donkelaar et al. estimate $PM_{2.5}$ by combining Aerosol Optical Depth (AOD) retrievals from the NASA's Medium Resolution Imaging Spectrometer (MODIS), Multi-angle Imaging Spectrometer (MISR), and Wide Field Ocean Observation Sensor (SeaWiFS) satellite instruments and coincident aerosol vertical profiles with the GEOS-Chem (<http://geos-chem.org/>, accessed on 10 March 2021) chemical transport model, and subsequently calibrated to regional ground-based observations using Geographically Weighted Regression (GWR) [49]. Ground-based $PM_{2.5}$ measurements over mainland China were obtained from <http://beijingair.sinaapp.com/>, accessed on 10 March 2021, Taiwanese $PM_{2.5}$ measurements were downloaded from <https://taqm.epa.gov.tw/taqm/tw/YearlyDataDownload.aspx>. For further details, see references [50,51]. These have been effectively applied to national and regional scale air pollution studies [9,52].

2.1.2. Land Use Dataset

Land use data originate from the CCI-LC global land cover product developed by the European Aviation Agency (<http://maps.elie.ucl.ac.be/CCI> accessed on 4 June 2020, 2020). The dataset covers the world with a time span of 1992–2018, of which the 2000–2015 data format is TIFF, the 2016–2018 data format is netCDF, the spatial resolution is 300 m, and the coordinate system is WGS-1984. ArcGIS 10.3.1 software and Chinese administrative boundaries are employed to tailor CCI-LC products and extract the land use data during 2000–2016. As the CCI-LC maps are designed to be globally consistent, the type of land counts 22 classes, and each class is associated with a ten values code. In this study, we re-combine the types of land use according to research needs. The classification rules are: urban areas of CCI-LC maps are reclassified into new urban land; water bodies of CCI-LC maps are reclassified into new water bodies; grassland of CCI-LC maps is reclassified into new grassland; cropland, rainfed and cropland, irrigated or post-flooding of CCI-LC maps are merged into new farmland; permanent snow and ice, bare areas, lichens and mosses of CCI-LC maps are merged into unused land; and the rest are classified as forest land.

2.2. Methods

2.2.1. Hot Spot Analysis (Getis-Ord G_i^*)

The hot spot analysis employed the Getis-Ord G_i^* [53,54] statistic to produce a hot (high $PM_{2.5}$ values) and cold (low $PM_{2.5}$ values) spot $PM_{2.5}$ pollution map. It is widely used in the analysis of the spatial agglomeration of geographic features. Getis-Ord G_i^* is formulated as:

$$G_i^* = \frac{\sum_{j=1}^n w_{i,j} x_j - \bar{X} \sum_{j=1}^n w_{i,j}}{\sqrt{\frac{\sum_{j=1}^n x_j^2}{n-1} - (\bar{X})^2} \sqrt{\frac{[n \sum_{j=1}^n w_{i,j}^2 - (\sum_{j=1}^n w_{i,j})^2]}{n-1}}} \quad (1)$$

where x_j is the $PM_{2.5}$ values for city j ; $w_{i,j}$ is the spatial weight between city i and j , the $w_{i,j}$ are constructed using the rook's case method (polygon features that share a boundary are neighbors); \bar{X} is the arithmetic average of x_j ; and n is equal to the total number of cities. The G_i^* statistic returned for each city is a z-score. For statistically significant (p -value) positive z-scores, the larger the z-score is, the more intense the clustering of high $PM_{2.5}$ values (hot spot). For statistically significant (p -value) negative z-scores, the smaller the z-score is, the more intense the clustering of low $PM_{2.5}$ values (cold spot). The p -value is a probability representing confidence levels [55], and in this study we set p -value equal to 0.05.

2.2.2. Semi-Parametric Spatial Durbin Model (SP-SDM)

The spatial lag model, spatial error model, and spatial Durbin model (SDM) are commonly used as spatial analysis tools [56,57]. As emissions from other neighboring areas affect $PM_{2.5}$ pollution levels, SDM can be applied to effectively measure its impact [31,56]. It can also be employed to measure the indirect effects of exogenous variables such as initial conditions and control variables in a region. Therefore, SDM is utilized in this manuscript

to analyze the relationship between $PM_{2.5}$ and land use change. However, the homogeneity of the investigated parameters is assumed in the traditional SDM [58]. The effects of explanatory variables on the explained variables are the same in all regions, and the spatial heterogeneity and non-linearity of regional growth behavior cannot be recognized [59]. In order to measure whether there are spatial heterogeneity and non-linear characteristics, two different forms of spatial econometric models are constructed through the generalized additive models (GAM) [60] and SDM for comparisons. $g_1(\mu)$ is an ordinary non-linear model, and $g_2(\mu)$ is SP-SDM, with the calculation formula as follows:

$$g_1(\mu) = \beta + \sum_i^m s(\alpha_i) + \varepsilon \quad i = 1, 2, \dots, m \quad (2)$$

$$g_2(\mu) = \beta + \sum_i^m s(\alpha_i, W\alpha_i) + s(WPM_{2.5}) + \varepsilon \quad i = 1, 2, \dots, m \quad (3)$$

where $g(\mu)$ is a link function, $\mu = E(PM_{2.5}/\alpha_1, \alpha_2, \dots, \alpha_m)$, β represents autoregressive coefficient, α_i represents the land use type, W is $n \times n$ order spatial weight matrix, and $K = 4$, $W\alpha_i$ and $WPM_{2.5}$ is the α_i and $PM_{2.5}$ spatial lag variables, respectively, ε is a random error, and $s(\cdot)$ is the smooth function of connecting explanatory variables. The *spdep* and *mgcv* packages in the R 3.6.3 version [61] (a free software environment for statistical computing and graphics) are used to calculate SP-SDM.

3. Results

3.1. Spatial and Temporal Pattern of $PM_{2.5}$

3.1.1. $PM_{2.5}$ Time Change Trend

The mean value of $PM_{2.5}$ in each city in China from 2000–2016 was calculated by the zonal statistics as table tool of ArcGIS 10.3.1 software. We consider the city-level vector boundary in China as the input feature zone data and the grid $PM_{2.5}$ data is used as the input value raster, with the statistics type set to mean. Finally, the mean value of the $PM_{2.5}$ concentration values of 369 cities was calculated from 2000 to 2016. The annual mean $PM_{2.5}$ for the whole of China is the average for all cities. Analysis results show the average value of $PM_{2.5}$ increased from $26.75 \pm 24.65 \mu\text{g}/\text{m}^3$ in 2000 to $31.23 \pm 25.08 \mu\text{g}/\text{m}^3$ in 2016, with an average annual growth rate of 0.97%. The minimum value appeared in 2000, and the maximum value of $38.46 \pm 31.40 \mu\text{g}/\text{m}^3$ appeared in 2014 in China.

With reference to the criterion value for the annual average concentration of $PM_{2.5}$, the target values for the three stages of a transition period, and the Chinese ambient air quality standards (GB3095-2012) set in the Air Quality Guidelines issued by the World Health Organization (WHO) in 2005, the annual average $PM_{2.5}$ is divided into five grades of $<10 \mu\text{g}/\text{m}^3$, $10\text{--}15 \mu\text{g}/\text{m}^3$, $15\text{--}25 \mu\text{g}/\text{m}^3$, $25\text{--}35 \mu\text{g}/\text{m}^3$, $>35 \mu\text{g}/\text{m}^3$. According to $PM_{2.5}$ classification rules, the $PM_{2.5}$ concentration values are classified and calculated to obtain the proportion of cities in different grades of $PM_{2.5}$ values, as shown in Figure 1. From 2000 to 2016, the proportion of cities with an annual average $PM_{2.5}$ concentration of less than $10 \mu\text{g}/\text{m}^3$ (criterion value) was 2.43–5.12%. The proportion of cities with an average yearly $PM_{2.5}$ concentration between 10 and $15 \mu\text{g}/\text{m}^3$ (IT-3: the annual average limit of target 3 in WHO transition period) was 3.77–8.63%. The proportion of cities with an average yearly $PM_{2.5}$ concentration between $15 \mu\text{g}/\text{m}^3$ and $25 \mu\text{g}/\text{m}^3$ (IT-2: the annual average limit of target 2 in WHO transition period) was 17.25–20.22%. The proportion of cities with an average yearly $PM_{2.5}$ concentration between $25 \mu\text{g}/\text{m}^3$ and $35 \mu\text{g}/\text{m}^3$ (IT-1: the annual average limit of target 1 in WHO transition period) was 23.18–25.34%. The proportion of cities with an annual average $PM_{2.5}$ concentration greater than $35 \mu\text{g}/\text{m}^3$ was 43.40–47.71%. The analysis showed that China's $PM_{2.5}$ governance had achieved certain results, but further efforts are needed to reduce $PM_{2.5}$ pollution and achieve sustainable development goals by 2035.

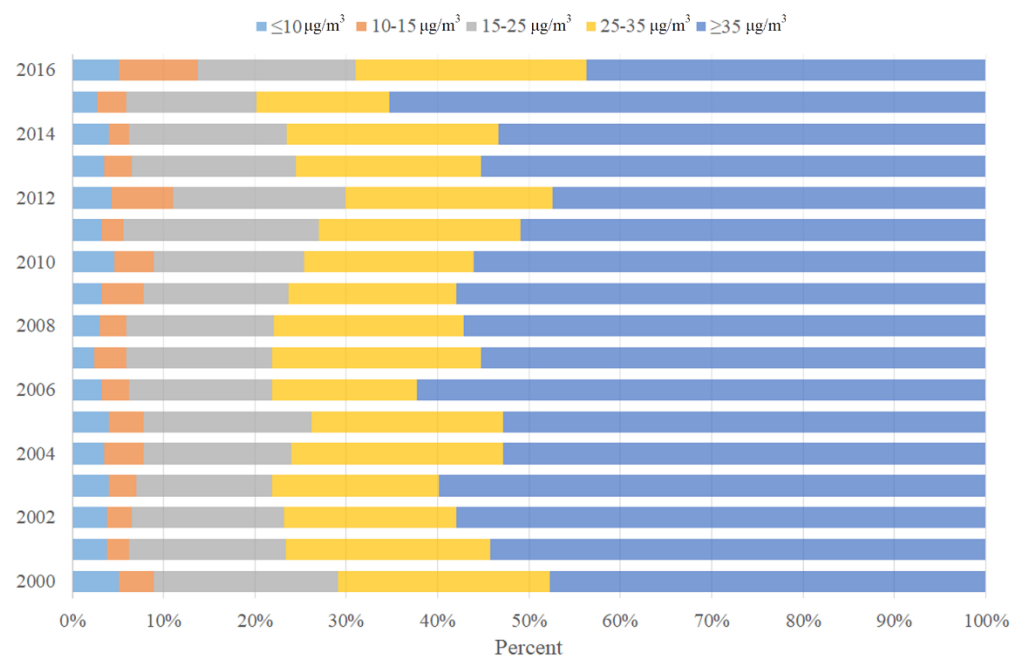


Figure 1. The proportion of cities within different PM_{2.5} value bins.

3.1.2. Spatial Distribution Pattern of PM_{2.5}

As can be seen from Figure 2, the spatial distribution of PM_{2.5} shows concentrated regional convergence, with obvious spatial heterogeneity. High PM_{2.5} values are shown in the densely populated and relatively economically developed central and eastern regions and the Taklimakan Desert in Xinjiang. In contrast, low PM_{2.5} values are mainly distributed in the west & central areas and south Fujian with low population density and relatively backward economic development. Except for natural factors, the spatial distribution pattern of PM_{2.5} is roughly consistent with that of the population and economic patterns, indicating that human socio-economic activities significantly impact PM_{2.5} concentration.

The hot spot analysis method was employed to identify the hot spots (high PM_{2.5} values) and cold spots (low PM_{2.5} values) of PM_{2.5} distribution in China and further analyze the clustering characteristics of PM_{2.5}. It is demonstrated that the spatial distribution of PM_{2.5} in China conforms to the characteristic analysis and clustering. Hot spots (high PM_{2.5} values) are mainly distributed in Kashgar, Aksu in western Xinjiang, the Beijing-Tianjin-Hebei region, Shandong Peninsula, the Central Plains, the middle reaches of the Yangtze River, the Yangtze River Delta, and other central and eastern urban agglomerations, especially the northern regions. They have experienced rapid industrialization and coal burning in winter, which has deteriorated air quality. Cold spots (low PM_{2.5} values) are mainly distributed in the north slope of the Tianshan Mountains, the Qinghai-Tibet Plateau, the west coast of the Taiwan Straits, the Yunnan-Guizhou Plateau, Hainan Province, and the border area between the three northeastern provinces and Inner Mongolia. From 2000 to 2016, most of the hot spots remained stable and only a few areas changed. The Chengdu-Chongqing Economic Zone and Lanzhou-Xining Urban Belt changed from hot spots to insignificant regions, indicating that air pollution has improved. The continuous expansion of cold spots (low PM_{2.5} values) in the urban agglomerations on the west coast of the Taiwan Straits, central Yunnan, and central Guizhou indicates that significant results have been achieved in air pollution control in these regions.

The spatial distribution of PM_{2.5} has strong heterogeneity due to different emission intensities of pollution gas and meteorological conditions in different areas of China, and different contributions by different types of PM_{2.5} precursors. PM_{2.5} pollutants in Xinjiang and Qinghai Qaidam Basin mainly came from sand dust aerosol. However, PM_{2.5} pollutants in eastern China and urban agglomerations mainly came from anthropogenic emissions. The reaction between nitrogen dioxide and sulfur dioxide in water absorbed by

PM_{2.5} is the main formation path of sulfate during fog and haze. Nitrogen oxides not only lead to an increase of PM_{2.5} concentration, but aerosols from high emissions of agriculture, industrial production, and airborne dust also results in the rapid generation of sulfates by their unique chemical pathways [38], which is one of the main reasons for the increased PM_{2.5} concentration.

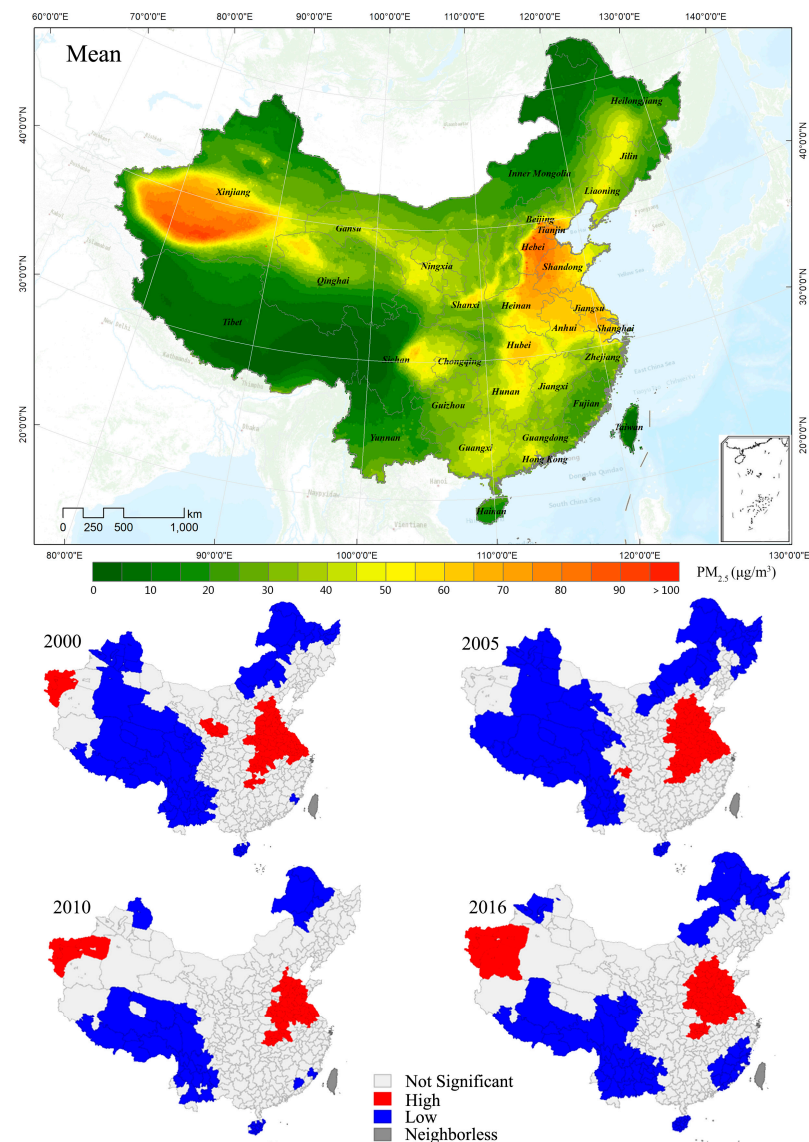


Figure 2. Mean spatial pattern and clustering of PM_{2.5} in China during 2000–2016.

3.2. PM_{2.5} Response to Land Use Change

3.2.1. Relationship between PM_{2.5} and Land Use Change

Land use space is the underlying surface of the atmospheric environment, which can directly or indirectly affect the temporal and spatial distribution pattern of PM_{2.5}. We calculated the land use area of different types in each city from 2000 to 2016 by ArcGIS software. The Spearman correlation coefficient method [62] is employed to determine the correlation between PM_{2.5} and land use types.

It is found that PM_{2.5} was positively correlated with urban land, farmland, and water bodies, and the correlation coefficients were 0.34 ($p = 0.01$), 0.047 ($p = 0.01$), and 0.067 ($p = 0.01$), respectively. PM_{2.5} was negatively correlated with forest land, grassland and unused land, and the correlation coefficients were -0.438 ($p = 0.01$), -0.265 ($p = 0.01$) and -0.441 ($p = 0.01$) respectively. Land use data were resampled to make its spatial resolution

consistent with the grid $PM_{2.5}$ data. Then, the mean concentration of $PM_{2.5}$ on different land types was calculated by using the resampled land use data of 2016. As shown in Figure 3, the average $PM_{2.5}$ concentrations show the highest values for urban land and decrease in the order of farmland > unused land > water body > forest > grassland. Because the unused land includes sandy land, dust in the desert is the cause of high $PM_{2.5}$ concentrations. The highest value being under urban land indicates the city as a major source area of $PM_{2.5}$ in China.

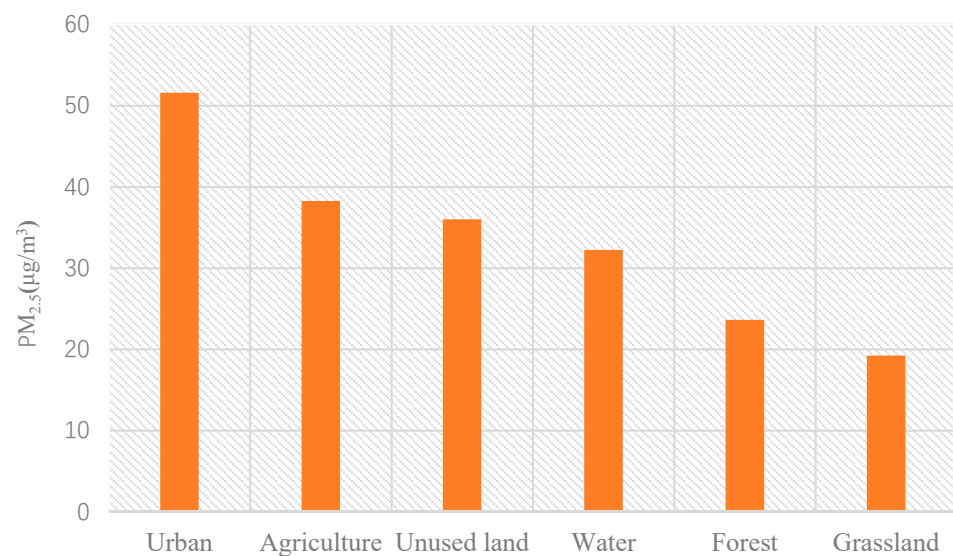


Figure 3. $PM_{2.5}$ values under different land use types.

3.2.2. Non-Linear Response of $PM_{2.5}$ to Land Use Change

The constructed SP-SDM was employed to measure the non-linear characteristics of $PM_{2.5}$ and land use change. To make the data more stable, logarithmic transformation was undertaken for land use types. The results are shown in Table 1. It was demonstrated that the two models have passed the 1% significance level test in terms of the estimated and referenced degrees of freedom. R^2 of model 2 is 0.86, which is significantly greater than that of model 1 (0.66). However, this shows the contrary values in Generalized Cross-Validation (GCV) [63]. The smaller the value of GCV, the better the performance of the model, indicating that the impact of land use change on $PM_{2.5}$ is statistically significant, and the fitting degree of SP-SDM is superior to that of the ordinary non-linear model. It can also be seen from Table 1 that the p -value of the spatial lag variables of $PM_{2.5}$ ($WPM_{2.5}$) is significant, indicating that $PM_{2.5}$ has a spatial spillover effect [56]. The degree of freedom for model 1 is greater than 1, showing that the function is a non-linear curve equation (when the degree of freedom is 1, the function is a linear equation) [60]. Moreover, the more significant non-linear relationship indicates the non-linear response of $PM_{2.5}$ concentration to land use changes.

The vertical axis in Figure 4 is the linear prediction value of $PM_{2.5}$, and the two horizontal axes are the land use type and its spatial lag variables respectively, reflecting the change characteristics of $PM_{2.5}$ concentration under the interaction of different land use scales and its spatial lag. In China, water bodies are mostly shown as long and narrow strips. Except for the northwest's sandy land, the unused land has a small distribution area in other places, especially on the urban fringe. This causes these two types of land to be prone to be polluted by adjacent land types. Therefore, the visual mapping is only performed for urban land, farmland, forest land, and grassland. It can be seen from Figure 5 that the $PM_{2.5}$ concentration value increases with the expansion of urban land and farmland and decreases with the expansion of forest land and grassland, indicating that the urban land and farmland have a positive contribution to $PM_{2.5}$ pollution. Forest land and grassland have a negative contribution to $PM_{2.5}$ pollution.

Table 1. Estimation results in SP-SDM.

| | | Edf/Coef | Ref.df | F | p-Value | R ² | GCV |
|-----------|---|----------|--------|--------------------------|--------------------------|----------------|--------|
| Model-1 | β_1 | 37.946 | / | / | $<2 \times 10^{-16}$ *** | | |
| | $s(\text{urban})$ | 8.420 | 8.906 | 51.69 | $<2 \times 10^{-16}$ *** | 0.66 | 97.695 |
| | $s(\text{farmland})$ | 8.816 | 8.989 | 128.39 | $<2 \times 10^{-16}$ *** | | |
| | $s(\text{forest})$ | 8.206 | 8.813 | 387.09 | $<2 \times 10^{-16}$ *** | | |
| | $s(\text{grassland})$ | 8.691 | 8.963 | 119.73 | $<2 \times 10^{-16}$ *** | | |
| | $s(\text{water})$ | 8.535 | 8.935 | 19.68 | $<2 \times 10^{-16}$ *** | | |
| | $s(\text{unused land})$ | 8.873 | 8.994 | 88.11 | $<2 \times 10^{-16}$ *** | | |
| β_2 | 37.946 | / | / | $<2 \times 10^{-16}$ *** | | | |
| Model-2 | $s(\text{urban}, W_{\text{urban}})$ | 26.662 | 28.65 | 18.945 | $<2 \times 10^{-16}$ *** | 0.86 | 41.438 |
| | $s(\text{farmland}, W_{\text{farmland}})$ | 28.266 | 28.95 | 34.535 | $<2 \times 10^{-16}$ *** | | |
| | $s(\text{forest}, W_{\text{forest}})$ | 27.706 | 28.88 | 101.210 | $<2 \times 10^{-16}$ *** | | |
| | $s(\text{grassland}, W_{\text{grassland}})$ | 27.848 | 28.89 | 42.595 | $<2 \times 10^{-16}$ *** | | |
| | $s(\text{water}, W_{\text{water}})$ | 25.543 | 28.25 | 9.445 | $<2 \times 10^{-16}$ *** | | |
| | $s(\text{unused land}, W_{\text{unused land}})$ | 27.229 | 28.78 | 21.305 | $<2 \times 10^{-16}$ *** | | |
| | $WPM_{2.5}$ | 8.039 | 8.76 | 471.029 | $<2 \times 10^{-16}$ *** | | |

Note: *** means p -value < 0.001 .

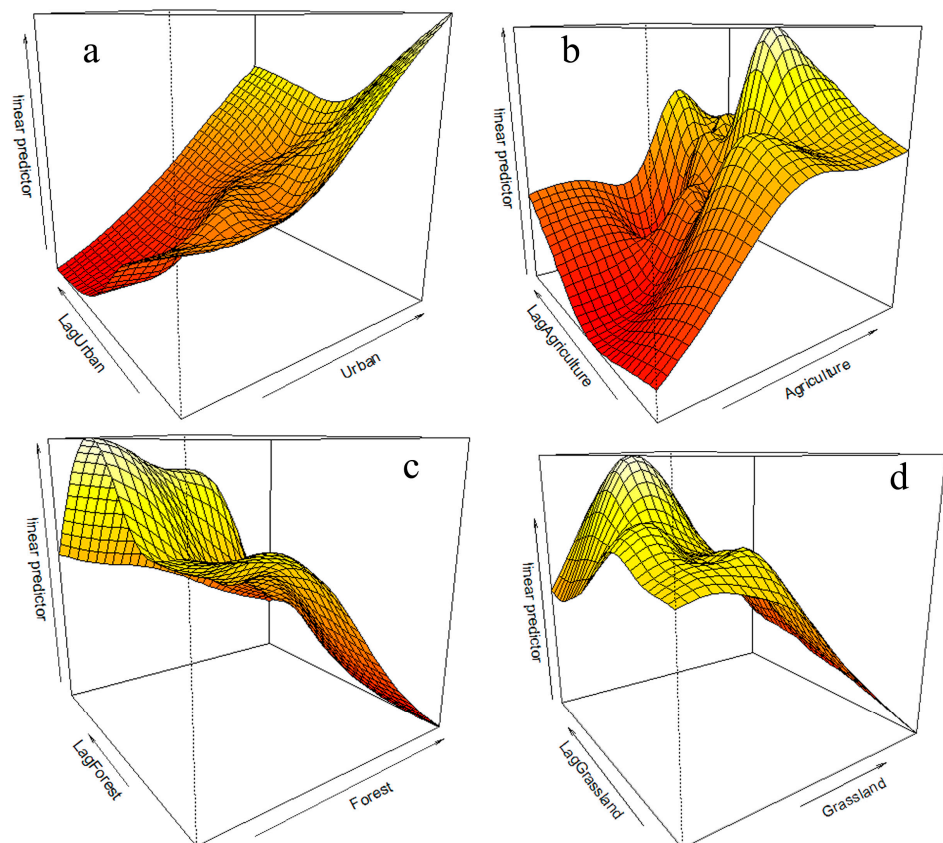


Figure 4. Three-dimensional effect graph of land use on the variation of $PM_{2.5}$ concentration. (a) urban; (b) agriculture; (c) forest; (d) grassland.

This is consistent with the above correlation analysis results. Generally, $PM_{2.5}$ decreases with the increase of the spatial lag of urban land, forest land, and grassland, while $PM_{2.5}$ increases with the increase of the spatial lag of farmland. Specifically, when the spatial lag of urban land expands, the $PM_{2.5}$ concentration almost decreases linearly. After the spatial lag of urban land reaches a high value, as the urban land continues to expand, the $PM_{2.5}$ concentration appears again rising trend. Unlike construction land, when the spatial lag of forest and grassland increases, the $PM_{2.5}$ concentration shows a trend from decline

to rise. When the spatial lag of forest and grassland reaches a high value, $PM_{2.5}$ shows a downward trend as the forest and grassland expand. It indicates that the expansion of urban land, forest land, and grassland in the surrounding area can suppress regional $PM_{2.5}$ pollution. However, as the local urban land scale expands, the construction scale in the surrounding regions also expands. This will increase $PM_{2.5}$ pollution. Air pollution in urban agglomerations in China is a typical phenomenon, indicating that urban land scale has an Environmental Kuznets Curve effect on $PM_{2.5}$ pollution. Reasonable control of the scale of urban land can achieve good environmental effects. Expansion of the forest land and grassland can not only suppress $PM_{2.5}$ pollution in the region, but it also has an inhibitory effect in adjacent areas. Moreover, the larger the scale of forest land and grassland, the more obvious the inhibitory effect. The large-scale and green production of farmland will help curb $PM_{2.5}$ pollution. The impact of land use scale on $PM_{2.5}$ pollution is a non-linear process, and different land use scales have different effects.

3.2.3. The Impact Mechanism of Land Use Change on $PM_{2.5}$ Pollution

As shown in Figure 5, as the main driver for air pollution, different land use types, patterns, and development intensities will obviously result in different distribution patterns of $PM_{2.5}$ pollution [64–67]. In fact, the expansion of urban scale and the increase in urban land area will lead to the imbalance of artificial and natural surface structures. In the process of this change, the land pattern has also changed. The construction of new residential areas, commercial areas, or industrial parks has improved the population density and commuting distance, thus increasing pollution emission sources. Changes in cities' landscape pattern structure have also changed the microclimate environment, which is prone to the heat island effect and increased water evapotranspiration [68]. In addition, the increase in land use and development intensity, building density, and height enable cities to accommodate more people. Still, it also increases the urban energy consumption, and the buildings are built higher and higher in the city. The effect of blocking and friction makes the wind flow through the city significantly weaker, thereby exacerbating $PM_{2.5}$ pollution [69]. On the contrary, the reasonable optimization of the land structure, distribution pattern, and development intensity can alleviate $PM_{2.5}$ pollution in the process of urban expansion.

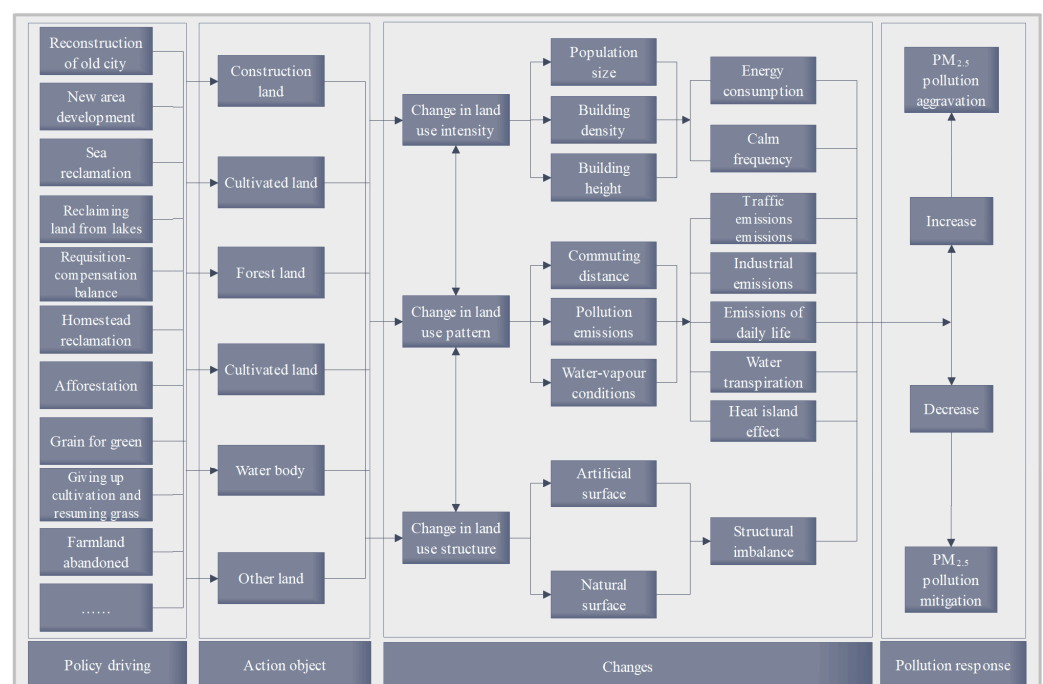


Figure 5. The impact mechanism of land use change on $PM_{2.5}$ pollution.

The area that can be used for newly-built green space and grassland is limited in cities. It is very difficult to control PM_{2.5} pollution by optimizing the land use structure alone. Government administrators will face the problem of where and how much to adjust. The city's real objective world is a three-dimensional space, and the distribution pattern and development intensity also affect the distribution pattern of PM_{2.5} pollution. Therefore, policy tools should be utilized for new urban development and urban reconstruction in old urban areas. Furthermore, the urban greening rate, the land use structure, development intensity, and distribution pattern should be gradually improved and optimized. The air duct should be reserved, and scattered ecological land shall be restored into an overall urban ecological network structure, which will exert a greater scale effect of ecological land. Thus, these improvements can play a role in reducing urban PM_{2.5} pollution.

4. Discussion

PM_{2.5} pollution is affected by both human-made and natural factors [70]. In the desert areas of northwest China, it is mainly affected by natural wind and dust [69]. However, it is mainly affected by human-made factors in eastern China, especially in urban agglomerations [3,31]. The empirical method of conditional mean regression has been employed in most of the existing studies. It cannot essentially reveal the differences in PM_{2.5} levels caused by the non-linearity and heterogeneity of different regions. SP-SDM is thus employed to effectively reveal the heterogeneity and non-linear impact mechanism of land use on PM_{2.5} and the interaction of land use and its spatial lag on PM_{2.5}. It is confirmed that PM_{2.5} pollution has a spatial spillover effect, and that the effects of different land use scales on PM_{2.5} are significantly different. It provides a certain reference for the management of PM_{2.5} pollution and the regional joint prevention and control of PM_{2.5} from the perspective of land use optimization. However, the "earth-atmosphere" system is a very complex system, and PM_{2.5} pollution is the result of the interaction, synergy, and coupling of natural conditions, human activities, and land use changes. Due to the difficulty in obtaining high-precision PM_{2.5} observational data and its complexity response to land use change, there are still many uncertainties. With the accumulation of high-precision PM_{2.5}, land use changes, and individual-based social and economic data, the response process and mechanism of PM_{2.5} pollution to land use changes should be focused on different time and space scales in the future.

5. Conclusions

Based on the remote sensing inversion of PM_{2.5} data and land use change data in long time series, the Getis-Ord G_i^* statistic and SP-SDM are employed to analyze the spatial distribution pattern of PM_{2.5} and its response to land use change. The main conclusions are as follows:

- (1) The average PM_{2.5} increased from 25.49 $\mu\text{g}/\text{m}^3$ to 31.23 $\mu\text{g}/\text{m}^3$ during 2000–2016, showing an annual average growth rate of 0.97%. It is still greater than 35 $\mu\text{g}/\text{m}^3$ in nearly half of the cities in China.
- (2) The spatial distribution pattern of PM_{2.5} presents the characteristics of concentrated regional convergence. PM_{2.5} is positively correlated with urban land and farmland, while it is negatively correlated with forest land, grassland, and unused land. Furthermore, the average PM_{2.5} concentrations show the highest values for urban land and decrease in the order of farmland > unused land > water body > forest > grassland.
- (3) The impact of land use change on PM_{2.5} is a non-linear process, and there are obvious differences for different land types. Moreover, it will also affect the surrounding areas. Thus, reasonably controlling the scale of urban land and farmland, optimizing the spatial distribution pattern and development intensity, and expanding the forest land and grassland are conducive to curbing PM_{2.5} pollution.

Author Contributions: Conceptualization, D.L., and W.X.; methodology, D.L.; Software, D.L.; validation, W.M.; formal analysis, D.L.; data curation, D.L., and W.M.; writing—original draft preparation, D.L. and W.M.; writing—review and editing, D.L. and L.Z.; visualization, D.L. and W.M.; supervision, D.L. All authors have read and agreed to the published version of the manuscript.

Funding: This research was sponsored by the Natural Science Foundation of Henan Province, grant number 202300410076.

Institutional Review Board Statement: Not applicable.

Informed Consent Statement: Not applicable.

Data Availability Statement: Not applicable.

Acknowledgments: Thanks Jing Wei for polishing the language, and thanks Dongyang Yang for providing funding supports.

Conflicts of Interest: The authors declare that they have no known competing financial interests or personal relationships that could have appeared to influence the work reported in this paper.

References

1. Han, L.; Zhou, W.; Li, W. City as a major source area of fine particulate (PM_{2.5}) in China. *Environ. Pollut.* **2015**, *206*, 183–187. [[CrossRef](#)]
2. Li, R.; Li, Z.; Gao, W.; Ding, W.; Xu, Q.; Song, X. Diurnal, seasonal, and spatial variation of PM_{2.5} in Beijing. *Sci. Bull.* **2015**, *60*, 387–395. [[CrossRef](#)]
3. Lu, D.; Mao, W.; Zheng, L.; Xiao, W.; Zhang, L.; Wei, J. Ambient PM_{2.5} Estimates and Variations during COVID-19 Pandemic in the Yangtze River Delta Using Machine Learning and Big Data. *Remote Sens.* **2021**, *13*, 1423. [[CrossRef](#)]
4. Chuanglin, F.; Fang, C.; Wang, S.; Sun, S. The Effect of Economic Growth, Urbanization, and Industrialization on Fine Particulate Matter (PM_{2.5}) Concentrations in China. *Environ. Sci. Technol.* **2016**, *50*, 11452–11459. [[CrossRef](#)]
5. Chen, B.; Li, S.; Yang, X.; Lu, S.; Wang, B.; Niu, X. Characteristics of atmospheric PM_{2.5} in stands and non-forest cover sites across urban-rural areas in Beijing, China. *Urban Ecosyst.* **2016**, *19*, 867–883. [[CrossRef](#)]
6. Song, C.; Wu, L.; Xie, Y.; He, J.; Chen, X.; Wang, T.; Lin, Y.; Jin, T.; Wang, A.; Liu, Y.; et al. Air pollution in China: Status and spatiotemporal variations. *Environ. Pollut.* **2017**, *227*, 334–347. [[CrossRef](#)]
7. Wang, S.; Zhou, C.; Wang, Z.; Feng, K.; Hubacek, K. The characteristics and drivers of fine particulate matter (PM_{2.5}) distribution in China. *J. Clean. Prod.* **2017**, *142*, 1800–1809. [[CrossRef](#)]
8. Yang, Y.; Quan, J.; Wang, Y.; Zhang, Y.; Cao, G.; Zhang, Q.; Wang, W.; Wang, J.; Sun, J.; Zhang, X.; et al. Factors contributing to haze and fog in China. *Chin. Sci. Bull.* **2013**, *58*, 1178–1187. (In Chinese) [[CrossRef](#)]
9. Lu, D.; Xu, J.; Yang, D.; Zhao, J. Spatio-temporal variation and influence factors of PM_{2.5} concentrations in China from 1998 to 2014. *Atmos. Pollut. Res.* **2017**, *8*, 1151–1159. [[CrossRef](#)]
10. Tian, S.; Pan, Y.; Liu, Z.; Wen, T.; Wang, Y. Size-resolved aerosol chemical analysis of extreme haze pollution events during early 2013 in urban Beijing, China. *J. Hazard. Mater.* **2014**, *279*, 452–460. [[CrossRef](#)]
11. Wang, Y.; Ying, Q.; Hu, J.; Zhang, H. Spatial and temporal variations of six criteria air pollutants in 31 provincial capital cities in China during 2013–2014. *Environ. Int.* **2014**, *73*, 413–422. [[CrossRef](#)]
12. Xue, W.; Zhang, J.; Zhong, C.; Ji, D.; Huang, W. Satellite-derived spatiotemporal PM_{2.5} concentrations and variations from 2006 to 2017 in China. *Sci. Total. Environ.* **2020**, *712*, 134577. [[CrossRef](#)]
13. Feng, B.; Li, L.; Xu, H.; Wang, T.; Wu, R.; Chen, J.; Zhang, Y.; Liu, S.; Ho, S.S.H.; Cao, J.; et al. PM_{2.5}-bound polycyclic aromatic hydrocarbons (PAHs) in Beijing: Seasonal variations, sources, and risk assessment. *J. Environ. Sci.* **2019**, *77*, 11–19. [[CrossRef](#)] [[PubMed](#)]
14. Wei, J.; Li, Z.; Lyapustin, A.; Sun, L.; Peng, Y.; Xue, W.; Su, T.; Cribb, M. Reconstructing 1-km-resolution high-quality PM_{2.5} data records from 2000 to 2018 in China: Spatiotemporal variations and policy implications. *Remote Sens. Environ.* **2021**, *252*, 112136. [[CrossRef](#)]
15. Zhu, G.; Hu, W.; Liu, Y.; Cao, J.; Ma, Z.; Deng, Y.; Sabel, C.E.; Wang, H. Health burdens of ambient PM_{2.5} pollution across Chinese cities during 2006–2015. *J. Environ. Manag.* **2019**, *243*, 250–256. [[CrossRef](#)] [[PubMed](#)]
16. Zhao, H.; Che, H.; Zhang, X.; Ma, Y.; Wang, Y.; Wang, H.; Wang, Y. Characteristics of visibility and particulate matter (PM) in an urban area of Northeast China. *Atmos. Pollut. Res.* **2013**, *4*, 427–434. [[CrossRef](#)]
17. Nguyen, G.T.H.; Shimadera, H.; Uranishi, K.; Matsuo, T.; Kondo, A. Numerical assessment of PM_{2.5} and O₃ air quality in Continental Southeast Asia: Impacts of potential future climate change. *Atmos. Environ.* **2019**, *215*, 116901. [[CrossRef](#)]
18. He, J.; Liu, H.; Salvo, A. Severe Air Pollution and Labor Productivity: Evidence from Industrial Towns in China. *Am. Econ. J. Appl. Econ.* **2019**, *11*, 173–201. [[CrossRef](#)]
19. Wang, G.; Cheng, S.; Li, J.; Lang, J.; Wen, W.; Yang, X.; Tian, L. Source apportionment and seasonal variation of PM_{2.5} carbonaceous aerosol in the Beijing-Tianjin-Hebei Region of China. *Environ. Monit. Assess.* **2015**, *187*, 1–13. [[CrossRef](#)]

20. Yu, L.; Wang, G.; Zhang, R.; Zhang, L.; Song, Y.; Wu, B.; Li, X.; An, K.; Chu, J. Characterization and Source Apportionment of PM_{2.5} in an Urban Environment in Beijing. *Aerosol Air Qual. Res.* **2013**, *13*, 574–583. [[CrossRef](#)]
21. Wang, G.; Zhang, R.; Gomez, M.E.; Yang, L.; Zamora, M.L.; Hu, M.; Lin, Y.; Peng, J.; Guo, S.; Meng, J.; et al. Persistent sulfate formation from London Fog to Chinese haze. *Proc. Natl. Acad. Sci. USA* **2016**, *113*, 13630–13635. [[CrossRef](#)]
22. Lv, L.; Chen, Y.; Han, Y.; Cui, M.; Wei, P.; Zheng, M.; Hu, J. High-time-resolution PM_{2.5} source apportionment based on multi-model with organic tracers in Beijing during haze episodes. *Sci. Total. Environ.* **2021**, *772*, 144766. [[CrossRef](#)] [[PubMed](#)]
23. Niu, Y.; Wang, F.; Liu, S.; Zhang, W. Source analysis of heavy metal elements of PM_{2.5} in canteen in a university in winter. *Atmos. Environ.* **2021**, *244*, 117879. [[CrossRef](#)]
24. Huang, Y.; Shen, H.; Chen, H.; Wang, R.; Zhang, Y.; Su, S.; Chen, Y.; Lin, N.; Zhuo, S.; Zhong, Q.; et al. Quantification of Global Primary Emissions of PM_{2.5}, PM₁₀, and TSP from Combustion and Industrial Process Sources. *Environ. Sci. Technol.* **2014**, *48*, 13834–13843. [[CrossRef](#)] [[PubMed](#)]
25. Shen, H.; Tao, S.; Chen, Y.; Ciais, P.; Güneralp, B.; Ru, M.; Zhong, Q.; Yun, X.; Zhu, X.; Huang, T.; et al. Urbanization-induced population migration has reduced ambient PM_{2.5} concentrations in China. *Sci. Adv.* **2017**, *3*, e1700300. [[CrossRef](#)]
26. Si, J.; Liu, X.; Xu, M.; Sheng, L.; Zhou, Z.; Wang, C.; Zhang, Y.; Seo, Y.-C. Effect of kaolin additive on PM_{2.5} reduction during pulverized coal combustion: Importance of sodium and its occurrence in coal. *Appl. Energy* **2014**, *114*, 434–444. [[CrossRef](#)]
27. Wang, Z.; Zhong, S.; He, H.-D.; Peng, Z.-R.; Cai, M. Fine-scale variations in PM_{2.5} and black carbon concentrations and corresponding influential factors at an urban road intersection. *Build. Environ.* **2018**, *141*, 215–225. [[CrossRef](#)]
28. Heald, C.L.; Geddes, J.A. The impact of historical land use change from 1850 to 2000 on secondary particulate matter and ozone. *Atmos. Chem. Phys. Discuss.* **2016**, *16*, 14997–15010. [[CrossRef](#)]
29. Dugord, P.-A.; Lauf, S.; Schuster, C.; Kleinschmit, B. Land use patterns, temperature distribution, and potential heat stress risk—The case study Berlin, Germany. *Comput. Environ. Urban Syst.* **2014**, *48*, 86–98. [[CrossRef](#)]
30. Huang, Z.; Du, X. Urban Land Expansion and Air Pollution: Evidence from China. *J. Urban Plan. Dev.* **2018**, *144*, 05018017. [[CrossRef](#)]
31. Lu, D.; Xu, J.; Yue, W.; Mao, W.; Yang, D.; Wang, J. Response of PM_{2.5} pollution to land use in China. *J. Clean. Prod.* **2020**, *244*, 118741. [[CrossRef](#)]
32. Wang, Y.; Zacharias, J. Landscape modification for ambient environmental improvement in central business districts—A case from Beijing. *Urban For. Urban Green.* **2015**, *14*, 8–18. [[CrossRef](#)]
33. Romero, H.; Ihl, M.; Rivera, A.; Zalazar, P.; Azocar, P. Rapid urban growth, land-use changes and air pollution in Santiago, Chile. *Atmos. Environ.* **1999**, *33*, 4039–4047. [[CrossRef](#)]
34. Marquez, L.O.; Smith, N.C. A framework for linking urban form and air quality. *Environ. Model. Softw.* **1999**, *14*, 541–548. [[CrossRef](#)]
35. Feng, H.; Zou, B.; Tang, Y. Scale- and Region-Dependence in Landscape-PM_{2.5} Correlation: Implications for Urban Planning. *Remote Sens.* **2017**, *9*, 918. [[CrossRef](#)]
36. Wu, J.; Xie, W.; Li, W.; Li, J. Effects of Urban Landscape Pattern on PM_{2.5} Pollution—A Beijing Case Study. *PLoS ONE* **2015**, *10*, e0142449. [[CrossRef](#)]
37. Anache, J.A.; Flanagan, D.C.; Srivastava, A.; Wendland, E.C. Land use and climate change impacts on runoff and soil erosion at the hillslope scale in the Brazilian Cerrado. *Sci. Total. Environ.* **2018**, *622–623*, 140–151. [[CrossRef](#)] [[PubMed](#)]
38. Alberti, M. The Effects of Urban Patterns on Ecosystem Function. *Int. Reg. Sci. Rev.* **2005**, *28*, 168–192. [[CrossRef](#)]
39. Seto, K.C.; Shepherd, J.M. Global urban land-use trends and climate impacts. *Curr. Opin. Environ. Sustain.* **2009**, *1*, 89–95. [[CrossRef](#)]
40. Shi, Y.; Ren, C.; Lau, K.K.-L.; Ng, E. Investigating the influence of urban land use and landscape pattern on PM_{2.5} spatial variation using mobile monitoring and WUDAPT. *Landsc. Urban Plan.* **2019**, *189*, 15–26. [[CrossRef](#)]
41. Zheng, S.; Zhou, X.; Singh, R.P.; Wu, Y.; Ye, Y.; Wu, C. The Spatiotemporal Distribution of Air Pollutants and Their Relationship with Land-Use Patterns in Hangzhou City, China. *Atmosphere* **2017**, *8*, 110. [[CrossRef](#)]
42. Yang, D.; Ye, C.; Wang, X.; Lu, D.; Xu, J.; Yang, H. Global distribution and evolvement of urbanization and PM_{2.5} (1998–2015). *Atmos. Environ.* **2018**, *182*, 171–178. [[CrossRef](#)]
43. Shi, K.; Wang, H.; Yang, Q.; Wang, L.; Sun, X.; Li, Y. Exploring the relationships between urban forms and fine particulate (PM_{2.5}) concentration in China: A multi-perspective study. *J. Clean. Prod.* **2019**, *231*, 990–1004. [[CrossRef](#)]
44. Shi, K.; Liu, C.; Huang, Y. Multifractal Processes and Self-Organized Criticality of PM_{2.5} during a Typical Haze Period in Chengdu, China. *Aerosol Air Qual. Res.* **2015**, *15*, 926–934. [[CrossRef](#)]
45. Qian, Z.; He, Q.; Lin, H.-M.; Kong, L.; Liao, D.; Dan, J.; Bentley, C.M.; Wang, B. Association of daily cause-specific mortality with ambient particle air pollution in Wuhan, China. *Environ. Res.* **2007**, *105*, 380–389. [[CrossRef](#)] [[PubMed](#)]
46. Gibson, M.D.; Kundu, S.; Satish, M. Dispersion model evaluation of PM_{2.5}, NO_x and SO₂ from point and major line sources in Nova Scotia, Canada using AERMOD Gaussian plume air dispersion model. *Atmos. Pollut. Res.* **2013**, *4*, 157–167. [[CrossRef](#)]
47. Mallia, D.V.; Lin, J.C.; Urbanski, S.P.; Ehleringer, J.R.; Nehrkorn, T. Impacts of upwind wildfire emissions on CO, CO₂, and PM_{2.5} concentrations in Salt Lake City, Utah. *J. Geophys. Res. Atmos.* **2015**, *120*, 147–166. [[CrossRef](#)]
48. Sulaymon, I.D.; Zhang, Y.; Hopke, P.K.; Zhang, Y.; Hua, J.; Mei, X. COVID-19 pandemic in Wuhan: Ambient air quality and the relationships between criteria air pollutants and meteorological variables before, during, and after lockdown. *Atmos. Res.* **2021**, *250*, 105362. [[CrossRef](#)]

49. Brunson, C.; Fotheringham, S.; Charlton, M. Geographically Weighted Regression. *J. R. Stat. Soc. Ser. D* **1998**, *47*, 431–443. [[CrossRef](#)]
50. Van Donkelaar, A.; Martin, R.V.; Li, C.; Burnett, R.T. Regional Estimates of Chemical Composition of Fine Particulate Matter Using a Combined Geoscience-Statistical Method with Information from Satellites, Models, and Monitors. *Environ. Sci. Technol.* **2019**, *53*, 2595–2611. [[CrossRef](#)]
51. Hammer, M.S.; Van Donkelaar, A.; Li, C.; Lyapustin, A.; Sayer, A.M.; Hsu, N.C.; Levy, R.C.; Garay, M.J.; Kalashnikova, O.V.; Kahn, R.A.; et al. Global Estimates and Long-Term Trends of Fine Particulate Matter Concentrations (1998–2018). *Environ. Sci. Technol.* **2020**, *54*, 7879–7890. [[CrossRef](#)]
52. Luo, J.; Du, P.; Samat, A.; Xia, J.; Che, M.; Xue, Z. Spatiotemporal Pattern of PM_{2.5} Concentrations in Mainland China and Analysis of Its Influencing Factors using Geographically Weighted Regression. *Sci. Rep.* **2017**, *7*, 40607. [[CrossRef](#)] [[PubMed](#)]
53. Ord, J.K.; Getis, A. Local Spatial Autocorrelation Statistics: Distributional Issues and an Application. *Geogr. Anal.* **1995**, *27*, 286–306. [[CrossRef](#)]
54. Getis, A.; Ord, J.K. The Analysis of Spatial Association by Use of Distance Statistics. In *Perspectives on Spatial Data Analysis*; Springer: Berlin/Heidelberg, Germany, 2010; pp. 127–145. [[CrossRef](#)]
55. Mitchel, A. *The ESRI Guide to GIS Analysis, Volume 2: Spatial Measurements and Statistics*; ESRI Press: Redlands, CA, USA, 2005; ISBN 158948116X.
56. Anselin, L.; Rey, S.J. *Modern Spatial Econometrics in Practice*; GeoDa Press LLC: Chicago, IL, USA, 2014.
57. Dubin, R.A. Spatial Autocorrelation: A Primer. *J. Hous. Econ.* **1998**, *7*, 304–327. [[CrossRef](#)]
58. Rey, S.J.; Montouri, B.D. US Regional Income Convergence: A Spatial Econometric Perspective. *Reg. Stud.* **1999**, *33*, 143–156. [[CrossRef](#)]
59. Basile, R. Regional economic growth in Europe: A semiparametric spatial dependence approach. *Pap. Reg. Sci.* **2008**, *87*, 527–544. [[CrossRef](#)]
60. Härdle, W.; Werwatz, A.; Müller, M.; Sperlich, S. *Generalized Additive Models*; CRC Press: Boca Raton, FL, USA, 1990; Volume 43. [[CrossRef](#)]
61. Team RC. *A Language and Environment for Statistical Computing*; R Foundation for Statistical Computing: Vienna, Austria, 2020; Available online: <http://www.R-project.org/> (accessed on 11 September 2020).
62. Croux, C.; Dehon, C. Influence functions of the Spearman and Kendall correlation measures. *J. Ital. Stat. Soc.* **2010**, *19*, 497–515. [[CrossRef](#)]
63. Golub, G.H.; Heath, M.; Wahba, G. Generalized Cross-Validation as a Method for Choosing a Good Ridge Parameter. *Technometrics* **1979**, *21*, 215–223. [[CrossRef](#)]
64. Nguyen, T.; Yu, X.; Zhang, Z.; Liu, M.; Liu, X. Relationship between types of urban forest and PM_{2.5} capture at three growth stages of leaves. *J. Environ. Sci.* **2015**, *27*, 33–41. [[CrossRef](#)]
65. Sun, L.; Wei, J.; Duan, D.; Guo, Y.; Yang, D.; Jia, C.; Mi, X. Impact of Land-Use and Land-Cover Change on urban air quality in representative cities of China. *J. Atmos. Solar-Terrestrial Phys.* **2016**, *142*, 43–54. [[CrossRef](#)]
66. Lu, D.; Mao, W.; Yang, D.; Zhao, J.; Xu, J. Effects of land use and landscape pattern on PM_{2.5} in Yangtze River Delta, China. *Atmos. Pollut. Res.* **2018**, *9*, 705–713. [[CrossRef](#)]
67. Xu, W.; Wu, Q.; Liu, X.; Tang, A.; Dore, A.J.; Heal, M.R. Characteristics of ammonia, acid gases, and PM_{2.5} for three typical land-use types in the North China Plain. *Environ. Sci. Pollut. Res.* **2016**, *23*, 1158–1172. [[CrossRef](#)] [[PubMed](#)]
68. Cao, C.; Lee, X.; Liu, S.; Schultz, N.; Xiao, W.; Zhang, M.; Zhao, C.C.X.L.S.L.W.X.M.Z.L. Urban heat islands in China enhanced by haze pollution. *Nat. Commun.* **2016**, *7*, 12509. [[CrossRef](#)]
69. Xu, J.; Zhou, G.; Xu, Z.; De Zhou, S.Z. Urban Haze Governance: Land Use Spatial Conflict and Governance Urban Air Duct. *China Land Sci.* **2015**, *29*, 51–58. [[CrossRef](#)]
70. Yang, D.; Wang, X.; Xu, J.; Xu, C.; Lu, D.; Ye, C.; Wang, Z.; Bai, L. Quantifying the influence of natural and socioeconomic factors and their interactive impact on PM_{2.5} pollution in China. *Environ. Pollut.* **2018**, *241*, 475–483. [[CrossRef](#)]